

A Secular Relativistic Model For Solar System's Numerical Simulations

Tabaré Gallardo^{1*} and Julia Venturini^{1†}

¹*Facultad de Ciencias, Instituto de Física, Iguá 4225, Montevideo, 11400, Uruguay*

5 February 2022

ABSTRACT

Using Gauss' averaged equations, we compute the secular relativistic effects generated by the Sun on the argument of the perihelion and the mean anomaly of an orbit. Then we test different alternative simpler models that have been proposed to reproduce the secular relativistic effects in the orbital elements. Generally, models introduce artificial perturbations that are velocity-independent but that depend on the heliocentric distance. If these perturbations are set as an impulse in a constant timestep integrator, when the particle approaches perihelion the generated impulse could be very strong and badly sampled, originating a spurious orbital evolution. In order to overcome this setback, we propose two new models based on a constant, distance-independent, perturbation. With these models we obtain the correct secular drift in the argument of perihelion and the expected secular orbital evolution is reproduced. We also discuss with some detail the secular effect generated on the mean anomaly by different models. This work is an expanded version of Venturini & Gallardo (2010).

Key words: Relativity – methods: numerical – celestial mechanics – comets – asteroids

1 INTRODUCTION

The problem of computing relativistic effects in planetary systems and in particular in the Solar System can be modeled by a perturbation to the Newtonian acceleration and is of increasing importance for future study of low perihelia and low semimajor axis populations. For our planetary system, the relevant relativistic effects are those generated by the Sun (see for example Benitez & Gallardo 2008). It is a usual practice in textbooks to show the relativistic effect in a planet's perihelion starting from a simplified problem that gives rise to a unique radial perturbation to the Newtonian potential conserving the angular momentum. But, a more rigorous analysis (Brumberg 1991; Shahid-Saless & Yeomans 1994; Bertotti et al. 2003) intended to agree with the IAU standards (Soffel et al. 2003) gives rise also to a transverse component and the expression for the relativistic perturbation becomes:

$$\Delta\ddot{\mathbf{r}} = \frac{\mu}{r^3 c^2} \left[\left(\frac{4\mu}{r} - \mathbf{v}^2 \right) \mathbf{r} + 4(\mathbf{v}\cdot\mathbf{r})\mathbf{v} \right] \quad (1)$$

where $\mu = k^2 m_\odot$ and \mathbf{r} , \mathbf{v} are heliocentric (Anderson et al. 1975; Quinn et al. 1991). This expression, that has no normal component, is valid when considering the relativistic effects generated only by a spherically symmetric and non rotating Sun. When the rotation of the Sun is considered a new effect called gravitomagnetic Lense-Thirring effect appears (Soffel 1989; Iorio 2005a). Furthermore, if all bodies have relativistic contributions a more complex expression should be used as explained in, for example, Benitez & Gallardo (2008). The time in Eq. (1) should be considered as the *coordinate time*; in order to compare with observables it is necessary to transform, for example, to Barycentric Coordinate Time (TCB) or Terrestrial Time (TT) (Shahid-Saless & Yeomans 1994; Soffel et al. 2003).

* E-mail: gallardo@fisica.edu.uy

† E-mail: jventurini@fisica.edu.uy

In order to avoid either the computational cost or the non symplectic form of Eq. (1), some simpler models that only depend on r have been proposed which mimic or reproduce the correct relativistic shift in the argument of the perihelia of the bodies under the gravitational effect of a central mass (Nobili & Roxburgh 1986; Saha & Tremaine 1992). But, as pointed out by Saha & Tremaine (1994), these models correctly recover the perihelion motion but fail in reproducing the evolution of the mean anomaly, M , point that we will discuss in this paper.

These r -dependent secular models have a disadvantage when used to compute high eccentricity low perihelion orbits in constant time-steps algorithms of the type “advance-impulse-advance”, as is the usual case in symplectic algorithms. In this case, the relativistic perturbation, when computed as an impulse, generates spurious results near the perihelion where the relativistic perturbation is stronger and poorly sampled. This is because the expression for the acceleration has a term that goes with $1/r^3$ and for low r values this impulse can be excessively high. For example, in the Solar System the relativistic perturbation for an asteroid at $r < 0.1$ AU is greater than the gravitational perturbation by Jupiter. Saha & Tremaine (1994), in a symplectic method for planetary integrations, incorporate part of the relativistic correction (1) in the “advance” part of the algorithm but an acceleration proportional to $1/r^3$ remains as part of the “impulse”.

In this paper we first review the relativistic effects on orbital elements with special attention to mean anomaly (Rubincam 1977; Calura et al. 1997; Iorio 2007). Then, we propose a very simple model that correctly reproduces the evolution of the argument of the perihelion, even for high eccentricity orbits, and which is very useful for symplectic or, more generally, constant timestep algorithms.

2 TIME AVERAGED GAUSS PLANETARY EQUATIONS

In order to compute the long term variations in the orbital elements produced by the perturbations it is a standard procedure to use the Gauss equations of planetary motion (Brumberg 1991; Murray & Dermott 1999; Beutler 2005). As we are interested in the secular evolution that these corrections generate, we calculate, in the first place, the Time Averaged Gauss Planetary Equations (TAGPE). To do so, we have to insert the radial, transverse, and normal components of the perturbing force (R , T and N respectively) into the Gauss equations, evaluate them on an unperturbed keplerian ellipse, integrate the equations over one orbital revolution (making use of the change of coordinates $dt = \frac{r^2}{h} df$) and divide them by the orbital period. So the mean variation rates are the following:

$$\begin{aligned}
 \langle \dot{a} \rangle &= \frac{1}{\sqrt{\mu a}(1-e^2)\pi} \int_0^{2\pi} \left[eR \sin f + T(1+e \cos f) \right] r^2 df \\
 \langle \dot{e} \rangle &= \frac{1}{2\pi\sqrt{\mu a^3}} \int_0^{2\pi} \left[R \sin f + T \left(\cos f + \frac{1}{e} \left(1 - \frac{r}{a} \right) \right) \right] r^2 df \\
 \langle \dot{i} \rangle &= \frac{1}{2\pi(1-e^2)\sqrt{\mu a^5}} \int_0^{2\pi} N \cos(f+\omega) r^3 df \\
 \langle \dot{\Omega} \rangle &= \frac{1}{2\pi(1-e^2)\sqrt{\mu a^5} \sin i} \int_0^{2\pi} N \sin(f+\omega) r^3 df \\
 \langle \dot{\omega} \rangle &= \frac{1}{2\pi e \sqrt{\mu a^3}} \int_0^{2\pi} \left[-R \cos f + T \sin f \left(\frac{2+e \cos f}{1+e \cos f} \right) \right] r^2 df - \cos i \langle \dot{\Omega} \rangle \\
 \langle \dot{M} \rangle &= \frac{-1}{\pi\sqrt{\mu a^5}(1-e^2)} \int_0^{2\pi} R r^3 df - \sqrt{1-e^2} (\langle \dot{\omega} \rangle + \langle \dot{\Omega} \rangle \cos i)
 \end{aligned} \tag{2}$$

where $r = \frac{a(1-e^2)}{1+e \cos f}$ and f is the true anomaly.

These expressions are valid assuming the orbital elements remain constant over an orbital period which is not strictly the case. For example, there exist very small amplitude periodic variations in the orbital elements generated by Eq. (1) (Richardson 1988) that have negligible effects on the Gauss equations except for the mean anomaly which is very sensitive to the variations of a . At Fig. 1 it is shown the variation of da/dt in one orbital period for Mercury due to Eq.(1). As the semimajor axis is not constant during one orbital period, the equation for $\langle \dot{M} \rangle$ should be considered as the secular relativistic effect on a body with a semimajor axis which has a mean value given by a .

3 RELATIVISTIC EFFECTS DUE TO THE CENTRAL STAR

The relativistic acceleration generated by a non rotating central massive body given by Eq. (1) can be decomposed in a radial (R) and transverse (T) components:

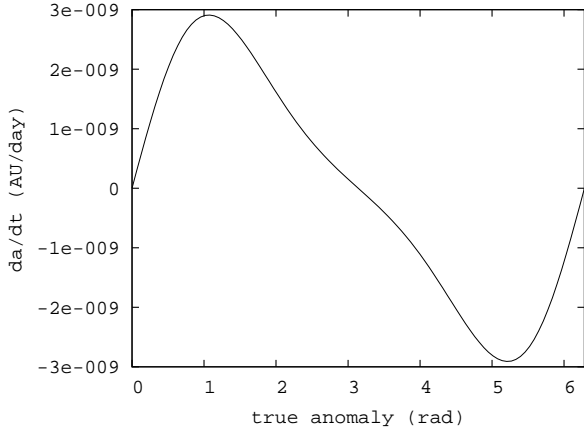


Figure 1. Daily variations in semimajor axis generated by Eq. (1) as deduced from the Gauss equations for planet Mercury. The relativistic perturbation induces an oscillation in the semimajor axis.

$$\begin{aligned}
 R &= \frac{\mu^2}{r^3 c^2} \left[2 + \frac{r}{a} \left(1 + \frac{4e^2}{1-e^2} \sin^2 f \right) \right] \\
 T &= \frac{4\mu^2 e \sin f}{c^2 r^3}
 \end{aligned} \tag{3}$$

(see also Damour & Daruelle 1985). Substituting in the TAGPE we can compute the secular variations of orbital elements produced by this acceleration:

$$\langle \dot{a} \rangle = \langle \dot{e} \rangle = \langle \dot{i} \rangle = \langle \dot{\Omega} \rangle = 0$$

$$\langle \dot{\omega} \rangle = \frac{3}{c^2(1-e^2)} \sqrt{\frac{\mu^3}{a^5}} \tag{4}$$

$$\langle \dot{M} \rangle = \frac{3}{c^2} \sqrt{\frac{\mu^3}{a^5}} \left(2 - \frac{5}{\sqrt{1-e^2}} \right) \tag{5}$$

where units are radians per day.

Eq. (4) is the well known relativistic effect on the argument of the perihelion and, for small eccentricities, Eq. (5) coincides, for example, with the approximate expressions for the secular drift in M given by Iorio (2005b) and with the secular drift in M generated by the relativistic model for low eccentricities used by Vitagliano (1997). The exact formula, valid for all eccentricities, is Eq. (5). We have checked this performing some numerical integrations with and without relativistic effects using the packages Mercury (Chambers 1999) and Evorb (Fernandez et al. 2002) of a system composed by only the Sun and a massless particle with the semimajor axis of Mercury and varying e from 0 to 0.9. (see Fig. 2). Some caution must be taken in computing $\langle \dot{M} \rangle$ by means of comparing two numerical integrations. Because of the oscillations on the semimajor axis generated by the relativistic correction, a particle integrated with the relativistic model is a particle that during the integration, on average, had a mean semimajor axis $\bar{a} \neq a_0$ being a_0 the initial value. Therefore, to compute the shift on M properly, one must compare the relativistic result with a classical integration in which the particle has a semimajor axis given by \bar{a} , not a_0 . Otherwise one would be comparing integrations of particles with different semimajor axes, and consequently, the obtained $\Delta M = M_{rel} - M_{cla}$ would be meaningless.

More problems arise when one wants to take into account the drift on mean anomaly of a specific real body in a numerical integration. The uncertainty Δa on the determination of the semimajor axis of real bodies generates an error in the mean motion ($\Delta n \simeq \sqrt{\mu/a^3} \Delta a$), which produces an uncertainty of the same order on the drift of mean anomaly. Setting $\Delta n \approx \langle \dot{M} \rangle$ and using Eq. (5), one finds that if

$$\Delta a \gtrsim \frac{3\mu}{c^2} \left(\frac{5}{\sqrt{1-e^2}} - 2 \right)$$

then the uncertainty on the osculating elements generates a secular drift on M greater than the relativistic effect itself. That means that for properly taking into account relativistic effect on M it is necessary to know with high precision, at least of the order of 10^{-8} AU for Solar System's bodies, the osculating semimajor axis. That is the case of the terrestrial planets from Mercury to Mars which have very well defined semimajor axes. On the contrary, the major planets have uncertainties significantly bigger (Pitjeva 2008). The relativistic effect in mean anomaly given by Eq. (5) and checked in our numerical tests

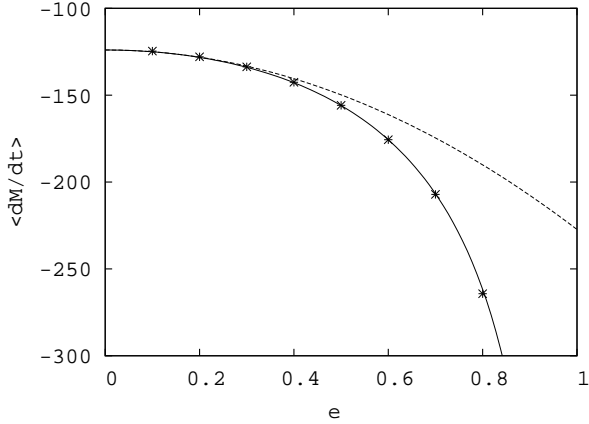


Figure 2. Secular relativistic effect on mean anomaly in arcsec/cy for a particle with Mercury’s semimajor axis. Full line: formula (5); dashed line: approximation for low eccentricity orbits (Iorio 2005b); dots: numerical results comparing two integrations with and without the relativistic perturbation given by Eq. (1).

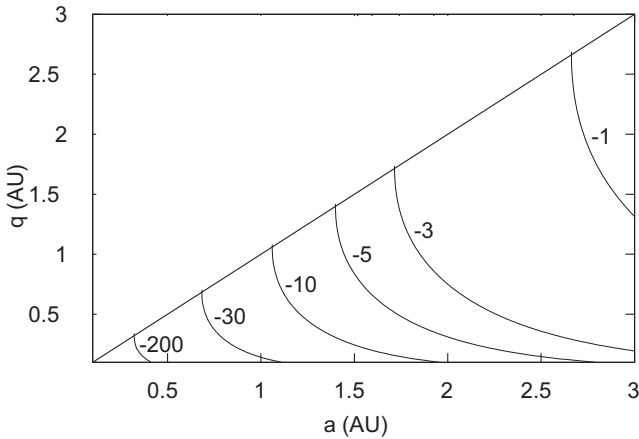


Figure 3. Relativistic effect on mean anomaly (arcsec/cy) according to formula (5) for a massless particle in the gravitational field of the Sun.

is showed in Fig. 3 as a function of the semimajor axis and perihelion distance. For comparison Fig. 4 shows the effect in ω given by Eq. (4).

4 MODELS THAT MIMIC THE SECULAR RELATIVISTIC EFFECTS

4.1 Proposed Models

If we are interested in computing the relativistic effects due to the Sun on a small body, we could just introduce Eq. (1) into an integrator. The problem is that this acceleration depends on both vectors position and velocity of the particle, so the speed of the integrator may be slowed down in order to calculate accurately the vectorial products at small heliocentric distances. Moreover, it is not a simple task to introduce this perturbation in a symplectic integrator, though it can be done (Saha & Tremaine 1994). In order to overcome this difficulty, some alternative simpler models have been created in the last two decades. The relativistic precession of the argument of perihelion is correctly reproduced defining a radial ($T = 0$) acceleration:

$$R = -\frac{6\mu^2}{c^2 r^3} \tag{6}$$

(Nobili & Roxburgh 1986). Inserting this R in the TAGPE the exact secular drifts generated by Eq. (1) are recovered except for mean anomaly. Saha & Tremaine (1992) added one more term into (6) in order to account for both ω and M drifts:

$$R = -\frac{6\mu^2}{c^2 r^3} + \frac{3\mu^2}{ac^2} \left(\frac{4}{\sqrt{1-e^2}} - 1 \right) \frac{1}{r^2} \tag{7}$$

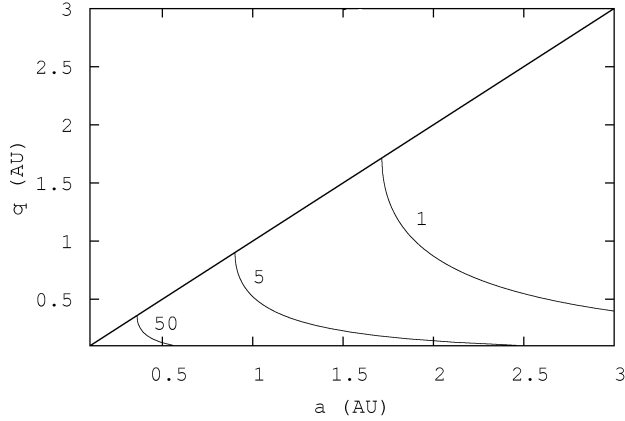


Figure 4. Relativistic effect on the argument of the perihelion (arcsec/cy) according to formula (4) for a massless particle in the gravitational field of the Sun.

Now, inserting this perturbation in the TAGPE, Eq. (4) and Eq. (5) are recovered. This apparent improvement to the original model of Nobili & Roxburgh (1986) is not so at all as pointed out by Saha & Tremaine (1994). The point is that given an initial osculating a_0 the mean \bar{a} generated by the evolution under Eq. (1) is different from the mean \bar{a}_R generated by the evolution under Eq. (7). Then, model (7) will not reproduce the secular evolution of an object with the correct \bar{a} but with a different mean semimajor axis given by \bar{a}_R . In consequence, the model introduces a secular drift in M and no evident progress is done in comparison with Eq. (6). This problem can be solved taking appropriate initial conditions as we explain in sec. 4.3.

4.2 Our r -independent Models

The corrections exposed above, though computationally better than Eq. (1) because the \mathbf{v} -dependance is eliminated; still have the problem that near perihelion the perturbation can be high enough to introduce numerical errors in constant time-step integrators.

One way of overcoming this difficulty is to look for a constant r -independent relativistic correction. To accomplish this task, we went back to Eq. (1), and assuming that the short period terms in the orbital elements do not affect the secular evolution of them, we time averaged the relativistic perturbation produced by a central body, obtaining:

$$\langle \Delta \ddot{\mathbf{r}} \rangle = -\frac{\mu^2}{c^2 a^3 \sqrt{(1-e^2)^3}} \mathbf{u}_e$$

where \mathbf{u}_e is the versor pointing to the pericenter. The fact that this averaged acceleration is a constant along \mathbf{u}_e , gave us the idea of trying with a constant perturbation in this direction. In order to obtain the same drift in ω as Eq. (4) using the TAGPE it is necessary to introduce a factor 2 and in terms of R and T can be written as

$$\begin{aligned} R &= -\frac{2\mu^2 e}{c^2 a^3 \sqrt{(1-e^2)^3}} \cos f \\ T &= \frac{2\mu^2 e}{c^2 a^3 \sqrt{(1-e^2)^3}} \sin f \end{aligned} \quad (8)$$

Inserting these expressions into the TAGPE, the elements a, e, i, Ω have zero variation and the mean variation in the ω is recovered, but for M we obtain:

$$\langle \dot{M} \rangle = -\frac{3(1+e^2)}{c^2} \sqrt{\frac{\mu^3}{a^5(1-e^2)^3}}$$

which is different from the real effect given by (5). Even so, one can also use a simpler constant radial perturbation ($T = 0$) that generates the expected variation in the argument of perihelion:

$$R = \frac{3\mu^2}{c^2 a^3 \sqrt{(1-e^2)^3}} \quad (9)$$

Again, from the TAGPE, the elements a, e, i, Ω have zero variation and the mean variation in the ω is recovered but for mean anomaly we obtain a different expression:

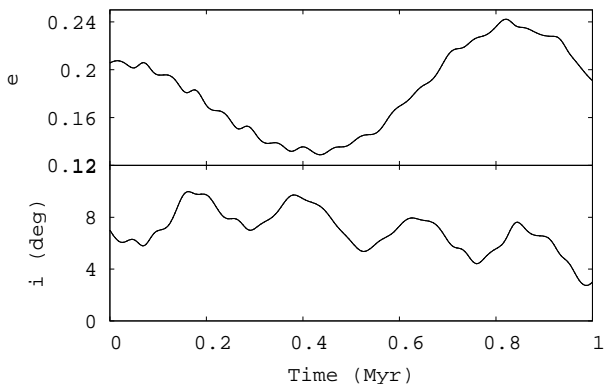


Figure 5. Results for planet Mercury from a Solar System’s relativistic numerical integration. Evolution of eccentricity and inclination according to models (1), (7) and (9). The numerical results of the all three different models coincide. A comparison with a non relativistic integration can be found in Benitez & Gallardo (2008).

$$\langle \dot{M} \rangle = -\frac{9}{c^2} \sqrt{\frac{\mu^3}{a^5(1-e^2)^3}} \quad (10)$$

but which is coincident with (5) for $e \rightarrow 0$. Therefore, with both constant models the drift in ω is recovered but there is a discrepancy for the drift in M . This is irrelevant in numerical simulations because, as we have explained, the predictions for M given by models cannot coincide with the true relativistic effect if the same set of initial conditions for all models are taken.

The last model that we propose (the constant radial acceleration) is somehow better than the one along \mathbf{u}_e because is computationally less demanding and also, in the case of low eccentricities, both Eq. (5) and Eq. (10) give the same result. Moreover, since model (9) only depends on (a, e) it is not necessary to evaluate the magnitude of the perturbation in each time step. The most important point is that model (9) maintains the precision of the numerical integration even for very small perihelion orbits while the original Eq. (1) needs a strong reduction in the step size.

4.3 On Initial Conditions

Initial conditions should be used according to the theory they were determined. For example, the model of Saha & Tremaine (1992) can be used confidently for generating precise ephemeris only if the initial conditions were obtained adjusting observations to this model. That is the underlying idea of the very accurate method for computing ephemeris of low eccentricity orbits proposed by Vitagliano (1997). But, it is not possible to follow the exact evolution of the mean anomaly if there is no consistence between the initial conditions (which they also should be very precise) and the model used. Then, any of the models we have analyzed are valid to follow the secular evolution of an orbit and, in particular, our constant radial perturbation model is computationally more convenient.

For illustrative purposes, in order to compare the variations of the orbital elements produced by the different models given by Eq. (1), Eq. (7) and Eq. (9), we integrated numerically our planetary system using Evorb for one million years. Results for planet Mercury are shown in Fig. 5 and Fig. 6. These figures corroborate what we have already stated by means of the Gauss equations: the secular relativistic evolution of all orbital elements is very well reproduced except for mean anomaly (a comparison with the classic evolution can be found in Benitez & Gallardo 2008). And even with strong differences in M (Fig. 6 bottom), the orbital evolution of the different models is almost undistinguishable. For example, at the end of the integration, differences of the order of 10^{-6} AU in a , 10^{-5} in e , 10^{-3} degrees on ω , 10^{-4} degrees on Ω , and even lower differences for i were obtained. Note also that the numerical deviations on M with respect to model (1) in Fig. 6 are mostly a consequence of using the same initial conditions for integrations that deal with different models. In the case of model (7), the drift on M will disappear if initial conditions consistent with this model are taken. In the case of model (9) some drift will persist.

5 CONCLUSIONS

By means of numerical integrations we confirmed the predicted secular drift in mean anomaly given by formula (5), which is valid for all eccentricities and was obtained introducing the relativistic effect due to the Sun (Eq. 1) into the time averaged Gauss’ planetary equations. Several models are able to reproduce the drift in ω but for high eccentricity orbits only the model

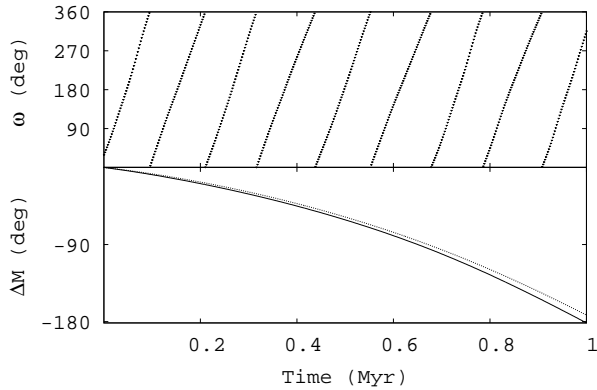


Figure 6. Top: evolution of Mercury’s argument of perihelion according to models (1), (7) and (9). All three models are coincident. Bottom: differences on Mercury’s mean anomaly between model (9) and (1) (full line) and between model (7) and (1) (dotted line). In spite of these differences the secular evolution is the same.

by Saha & Tremaine (1992) can follow the exact secular drift in M and only if appropriate initial conditions are taken. For secular evolution studies of numerous populations by means of numerical integrations, if no precise ephemeris are required, our constant radial independent model is very convenient, specially if low perihelion orbits are involved. For accurate ephemeris computations of real bodies, the original formula (1) or even the full relativistic N-body one should be used with a control of the integrator’s precision in the case of low perihelion orbits.

ACKNOWLEDGMENTS

J. Venturini acknowledges a scholarship from PEDECIBA. This work was done as part of the Project “Caracterización de las poblaciones de cuerpos menores del sistema solar” (ANII). We acknowledge comments by anonymous referees.

REFERENCES

- Anderson, J.D., Esposito, P.B., Martin, W. & Muhlemsn, D.O., 1975, *Astrophys. J.*, 200, 221
 Benitez, F. & Gallardo, T., 2008, *Celest. Mech. and Dyn. Ast.*, 101, 289
 Bertotti, B., Farinella, P. and Vokrouhliký, D., 2003, *Physics of the Solar System*. Kluwer Academic Publishers, p.557
 Beutler, G., 2005, *Methods of Celestial Mechanics*. First ed., Springer, p.230
 Brumberg, V., 1991, *Essential Relativistic Celestial Mechanics*. Adam Hilger, London. ISBN 0-7503-0062-0
 Calura, M., Fortini, P. and Montanari, E., 1997, *Phys. Rev. D*, 56, 4782
 Chambers, J.E., 1999, *MNRAS* 304, 793
 Damour, T. and Daruelle, N., 1985, *Annales de l’ I.H.P. section A*, 43(1), 107
 Fernandez, J.A., Gallardo, T. & Brunini, A., 2002, *Icarus* 159, 358
 Iorio, L., 2005a, *A&A* 431, 385
 Iorio, L., 2005b, *A&A* 433, 385
 Iorio, L., 2007, *ApSS*, 312, 331
 Iorio, L., 2008, *Advances in The Measurement of the Lense-Thirring Effect with Planetary Motions in the Field of the Sun*. Scholarly Research Exchange, ID 105235
 Murray C., Dermott F., 1999, *Solar System Dynamics*, First ed., Cambridge Univ. Press, p. 54
 Newhall, X.X., Standish, E.M. & Williams, J.G., 1983, *A&A* 125, 150
 Nobili, A. & Roxburgh, I., 1986, *Simulation of Relativistic Corrections in Long Term Numerical Integrators of Planetary Orbits*. In “Relativity in Celestial Mechanics and Astronomy”, ed. by J. Kovalevsky and V.A. Brumberg, 105
 Pitjeva, E. V., 2008, *Use of optical and radio astrometric observations of planets, satellites and spacecraft for ephemeris astronomy*, in *A Giant Step: from Milli- to Micro-arcsecond Astrometry*, Proceedings of the International Astronomical Union, IAU Symposium, Volume 248, p. 20
 Quinn, T., Tremaine, S. & Duncan, M., 1991, *Astron. J.* 101, 2287
 Richardson, D. L., 1988, *Cel. Mech.*, 43, 193
 Rubincam, D. P., 1977, *Cel. Mech.*, 15, 21

Saha, P. & Tremaine, S., 1992, *Astron. J.* 104, 1633

Saha, P. & Tremaine, S., 1994, *Astron. J.* 108, 1962

Shahid-Saless, B. & Yeomans, D., 1994, *Astron. J.* 107, 1885

Soffel, M., 1989, *Relativity in Astrometry, Celestial Mechanics and Geodesy*, Springer

Soffel, M.; Klioner, S. A.; Petit, G.; Wolf, P.; Kopeikin, S. M.; Bretagnon, P.; Brumberg, V. A.; Capitaine, N.; Damour, T.; Fukushima, T.; Guinot, B.; Huang, T.-Y.; Lindgren, L.; Ma, C.; Nordtvedt, K.; Ries, J. C.; Seidelmann, P. K.; Vokrouhlick, D.; Will, C. M.; Xu, C., 2003, *Astron. J.* 126, 6, 2687

Venturini, J. & Gallardo, T., 2010, in "Icy Bodies of the Solar System", *Proceedings of the International Astronomical Union, IAU Symposium, Volume 263*, p. 106

Vitagliano, A., 1997, *Celest. Mech. and Dyn. Ast.* 66, 293